AIAA JOURNAL
Vol. 35, No. 7, July 1997

Active Control of Turbomachine Discrete Frequency Noise Utilizing Oscillating Flaps and Pistons

Jason A. Minter* and Sanford Fleeter†
Purdue University, West Lafayette, Indiana 47907

Turbomachine discrete frequency tones are a significant environmental concern. These tones are generated by periodic blade row interactions, with only specific circumferential acoustic modes generated. This research is directed at active control of discrete frequency noise generated by subsonic blade rows through cancellation of the propagating acoustic waves, accomplished by utilizing airfoil surface mounted oscillating actuators to generate additional control propagating pressure waves. These control waves interact with the propagating acoustic waves, thereby canceling the acoustic waves and thus the far-field discrete frequency tones. A series of experiments are described, directed at investigating the fundamentals of this active discrete frequency noise control technique as well as verifying basic modeling assumptions. Both an isolated vane and a three-vane row are utilized, with the stator vane actuators including both oscillating flaps and surface pistons.

Nomenclature

a_∞	= speed of sound
C/S	= cascade solidity
h	= h_{piston} is the piston amplitude, $h_{\text{piston}}e^{i\omega t}$
k_c	= reduced frequency
k_θ	= tangential wave number
k_ξ	= axial wave number
M	= freestream Mach number
M_θ	= tangential Mach number, $M \sin\Theta$
M_ξ	= axial Mach number, $M \cos\Theta$
m	= mode number
N_{blades}	= number of rotor blades
N_{vanes}	= number of stator vanes
n	= rotor harmonic
p	= perturbation pressure
$\bar{p}$	= complex pressure perturbation constant
q_{piston}	= piston velocity, $\mathrm{d}h/\mathrm{d}t$
U_∞	= mean axial velocity
u	= axial perturbation velocity
$\bar{u}$	= complex velocity perturbation constant parallel to blade row
V_∞	= mean tangential velocity
v	= tangential perturbation velocity
$\bar{v}$	= complex velocity perturbation constant normal to blade row
$w_{\text{G,LE}}$	= vortical gust velocity magnitude at the airfoil leading edge
$w(x)$	= airfoil surface upwash velocity
x	= direction along chord
y	= direction normal to chord
α_{flap}	= flap torsion amplitude
Θ	= cascade stagger angle
θ	= tangential coordinate
ξ	= axial coordinate
ϕ	= phase angle between the actuator motion and the vortical gust
Ω	= rotor rotational speed
ω	= frequency

Received May 7, 1996; revision received Feb. 20, 1997; accepted for publication March 1, 1997.

*Research Assistant, School of Mechanical Engineering. Student Member AIAA.

†McAllister Distinguished Professor, School of Mechanical Engineering. Associate Fellow AIAA.

Introduction

AEROACOUSTICS is an increasingly important issue in the design of high-performance gas turbine engines, with discrete frequency tones being a significant environmental concern. These discrete frequency tones are generated by periodic blade row unsteady aerodynamic interactions. Namely, turbomachine blade rows are subject to spatially nonuniform inlet flowfields resulting from, for example, inlet distortions or the wakes from upstream airfoil rows. The interaction of a downstream airfoil row with these nonuniform spatial inlet flows results in periodic unsteady aerodynamic forces on the downstream blading, which are the source of the discrete frequency tones. The discrete tones appear in an engine noise spectrum as spikes at multiples of blade passing frequency, whose magnitudes are significantly higher than the background broadband noise levels.

One noise control approach involves cancellation of the unsteady aerodynamic forces on the airfoil, the unsteady lift, thereby decreasing the noise generation,[1] accomplished, for example, with oscillating flaps.[2,3] Although appropriate for isolated airfoils, this is not a first principals approach for turbomachine blade rows. Namely, blade row interactions generate acoustic waves that may propagate unattenuated or decay exponentially with distance, depending on the rotor stator relative airfoil counts as just described. If decaying perturbations are produced, the mode is said to be cut off, with no far-field discrete frequency noise generated. In contrast, with a propagating mode, a pair of acoustic waves are formed, one traveling upstream and the other downstream, resulting in far-field discrete frequency tones.

For a turbomachine stage, only specific circumferential acoustic modes are generated by the rotor–stator interaction, with these modes determined by the number of rotor blades and stator vanes. Only some of these modes propagate to the far field, with the rest decaying before reaching the far field. To decrease the far-field discrete frequency noise, the propagating acoustic pressure modes must be controlled. There are two approaches: cancellation of the duct mode or cancellation of the mode generation source.

With duct mode cancellation, the propagating pressure modes are canceled in the engine ducts. This technique has potential but also some difficulties. For example, the cancellation mechanism is mounted external to the duct, i.e., on the inner or outer duct radii. Hence, it is very difficult to cancel propagating acoustic pressure circumferential modes with radial components. Using duct-mounted loud speakers and generating only plane waves, active noise control was demonstrated by Thomas et al.[4] on a JT15D turbofan engine, with a decrease in the fundamental tone of up to 16 dB achieved. The noise was decreased for a range of ± 30 deg about the engine axis but was increased for all other angles, with a maximum increase of 15 dB. Thus, this noise control technique is not effective over the entire engine inlet region.

Mode generation source cancellation is accomplished by generating additional control propagating pressure waves that interact with those generated by the rotor–stator interaction, thereby providing the physical mechanism for the far-field discrete frequency noise control. Ideally, these additional control propagating waves will cancel the rotor–stator generated propagating waves, both upstream and downstream, thereby resulting in no propagating acoustic modes and thus no far-field discrete frequency tones. In this approach, initially proposed by Kousen and Verdon,[5] a computational model based on LinFlo[6] was developed for controlling wake–blade interaction noise by means of oscillating pistons. Later, Minter et al.[7] developed an analogous model based on LinSub,[8] directed at actuator requirements for oscillating leading- and trailing-edge flaps as well as surface pistons. Note that this propagating wave cancellation approach does not correspond to unsteady lift cancellation because the unsteady lift is a result of both the propagating and nonpropagating waves.

This research is directed at active control of discrete frequency noise generated by subsonic blade rows through cancellation of the propagating acoustic waves, accomplished by utilizing airfoil surface mounted oscillating actuators to generate additional control propagating pressure waves. These control waves interact with the propagating acoustic waves, thereby, in principle, canceling the acoustic waves and thus the far-field discrete frequency tones. A series of experiments, directed at investigating the fundamentals of this active discrete frequency noise control technique as well as verifying basic math model assumptions, are described. Both an isolated vane and a three-vane row are utilized, with the stator vane actuators including both oscillating flaps and surface pistons.

Discrete Frequency Noise Generation

The model to analyze the discrete frequency noise generated in a turbomachine considers a rotor and stator in a duct, with the flow inviscid and compressible with small unsteady perturbations, described by the three-dimensional wave equation

$$\left(\frac{\partial}{\partial t}+U_\infty\frac{\partial}{\partial \xi}\right)^2 p = a_\infty^2\left(\frac{\partial^2}{\partial r^2}+\frac{1}{r}\frac{\partial}{\partial \xi}+\frac{1}{r^2}\frac{\partial^2}{\partial \theta^2}+\frac{\partial^2}{\partial \xi^2}\right)p \quad (1)$$

This wave equation is variable, separable, and harmonic in time, with solution

$$p(\xi, r, \theta, t) = \bar{p}(r)\exp[i(k_\xi \xi + k_\theta \theta - n N_{\text{blades}}\Omega t)] \quad (2)$$

where $\omega = n N_{\text{blades}}\Omega$, and k_θ is the mode order, corresponding to the number of nodal diameters of the pressure pattern.

Tangential Wave Number k_θ

The duct acoustic modes are generated by the unsteady pressures generated by N_{blades} rotor blades rotating at speed Ω interacting with N_{vanes} downstream stationary vanes. The vane tangential spacing $\Delta\theta$ is equal to $\Delta\theta = 2\pi/N_{\text{vanes}}$, with the vanes indexed $v = 1, 2, \ldots, N_{\text{vanes}}$. In time $t \longrightarrow t + (\Delta\theta/\Omega)$, the rotor will traverse one stator passage so that the rotor position goes to $\theta \longrightarrow \theta + \Delta\theta$; see Fig. 1. The response of the $v = 2$ vane is

$$p(\xi, r, \theta+\Delta\theta, t+\Delta t) = \bar{p}(r)\exp\left\{i\left[k_\xi\xi + k_\theta\left(\theta+\frac{2\pi}{N_{\text{vanes}}}\right) - nBN_{\text{blades}}\Omega\left(t+\frac{2\pi}{N_{\text{Vanes}}\Omega}\right)\right]\right\} \quad (3)$$

With the rotor in this position, the response of the $v = 2$ stator is identical to the response of the $v = 1$ stator at time t:

$$\bar{p}(r)\exp[i(k_\xi\xi + k_\theta\theta - n N_{\text{blades}}\Omega t)] = \bar{p}(r)\exp\left\{i\left[k_\xi\xi + k_\theta\left(\theta+\frac{2\pi}{N_{\text{vanes}}}\right) - nN_{\text{blades}}\Omega\left(t+\frac{2\pi}{N_{\text{vanes}}\Omega}\right)\right]\right\} \quad (4)$$

and

$$e^{i\left(k_\theta\frac{2\pi}{N_{\text{vanes}}} - nN_{\text{blades}}\Omega\frac{2\pi}{N_{\text{vanes}}\Omega}\right)} = e^{i(2\pi m)}$$

where m is any integer. Solving for k_θ,

$$k_\theta = n N_{\text{blades}} + m N_{\text{vanes}} \qquad m = \pm 1, \pm 2, \pm 3, \ldots \quad (5)$$

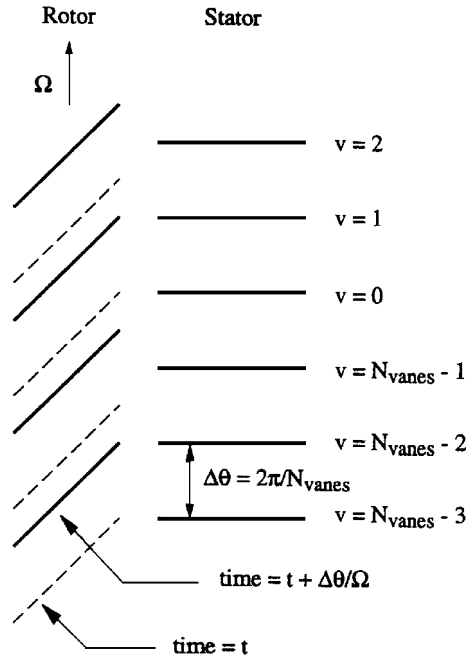

Fig. 1 Cascade periodicity in time and space.

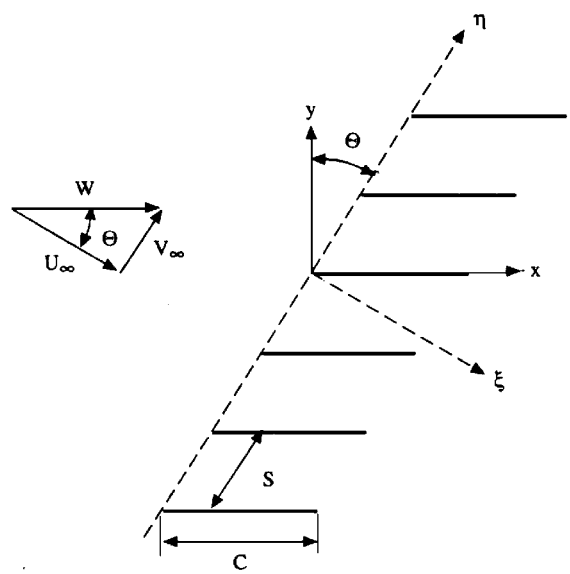

Fig. 2 Mean flow and cascade geometry.

Thus, the only modes generated by the rotor–stator interaction are specified by the values of k_θ. The frequencies are the harmonics of blade pass $\omega = n N_{\text{blades}}\Omega$, with the acoustic duct modes also responding at these frequencies. The phase speed $\Omega_p = n N_{\text{blades}}\Omega/k_\theta$ is the angular velocity of the (k_θ, n)th pressure mode. Note that a negative value for m represents a backward traveling wave.

Axial Wave Number k_ξ

The linear theory model to analyze rotor–stator interactions considers a two-dimensional flat plate cascade in a subsonic inviscid isentropic irrotational flowfield (Fig. 2). The unsteady flow is assumed to be a small perturbation to the uniform mean flow, leading to the following linearized continuity and momentum equations:

$$\frac{\partial p}{\partial t}+U_\infty\frac{\partial p}{\partial \xi}+V_\infty\frac{\partial p}{\partial \theta}+\rho_\infty A_\infty^2\left(\frac{\partial u}{\partial \xi}+\frac{\partial v}{\partial \theta}\right)=0$$

$$\frac{\partial u}{\partial t}+U_\infty\frac{\partial u}{\partial \xi}+V_\infty\frac{\partial u}{\partial \theta}+\frac{1}{\rho_\infty}\frac{\partial p}{\partial \xi}=0 \quad (6)$$

$$\frac{\partial v}{\partial t}+U_\infty\frac{\partial v}{\partial \xi}+V_\infty\frac{\partial v}{\partial \theta}+\frac{1}{\rho_\infty}\frac{\partial p}{\partial \theta}=0$$

The unsteady flow is harmonic in space and time:

$$\begin{bmatrix} u(\xi,\theta,t) \\ v(\xi,\theta,t) \\ p(\xi,\theta,t) \end{bmatrix} = \begin{bmatrix} \bar{u} \\ \bar{v} \\ \bar{p} \end{bmatrix} \exp[i(k_\xi \xi + k_\theta \theta - \omega t)] \tag{7}$$

where the discrete frequency acoustic or pressure waves are defined by the complex wave strength $\bar{p}$ and the axial and tangential wave numbers k_ξ and k_θ.

Substituting into the linearized continuity and momentum equations

$$\begin{bmatrix} (U_\infty k_\xi + V_\infty k_\theta - \omega) & A^2_\infty k_\xi \rho_\infty & A^2_\infty k_\theta \rho_\infty \\ k_\xi/\rho_\infty & (U_\infty k_\xi + V_\infty k_\theta - \omega) & 0 \\ k_\theta/\rho_\infty & 0 & (U_\infty k_\xi + V_\infty k_\theta - \omega) \end{bmatrix} \times \begin{bmatrix} \bar{p} \\ \bar{u} \\ \bar{v} \end{bmatrix} = 0 \tag{8}$$

For a nontrivial solution, the determinant of the coefficients must be zero, leading to the following characteristic equation:

$$(U_\infty k_\xi + V_\infty k_\theta - \omega)[(U_\infty k_\xi + V_\infty k_\theta - \omega)^2 - A^2_\infty (k^2_\xi + k^2_\theta)] = 0 \tag{9}$$

There are two families of solutions: a vorticity wave and two acoustic waves. The acoustic wave characteristics are determined by k_θ, with k_ξ describing whether the waves propagate unattenuated or decay.

The axial wave numbers k_ξ are calculated from the respective solutions of the characteristic equation. The solution corresponds to a pair of irrotational acoustic or pressure waves, one propagating upstream and the other downstream at the speed of sound if $(U_\infty k_\xi + V_\infty k_\theta - \omega)^2 - A^2_\infty (k^2_\xi + k^2_\theta) = 0$. The terms k_ξ for these pressure waves are

$$k_\xi = \frac{M_\xi (k_\theta M_\theta - \omega/A_\infty) \pm \sqrt{(k_\theta M_\theta - \omega/A_\infty)^2 - (1 - M^2_\xi) k^2_\theta}}{1 - M^2_\xi} \tag{10}$$

Far-Field Discrete Frequency Noise

Although all of the acoustic pressure circumferential modes of order $k_\theta = nN_{\text{blades}} + mN_{\text{vanes}}$ are generated by the rotor–stator interaction at the harmonics of blade passage frequency $\omega = nN_{\text{blades}}\Omega$, only certain of these modes propagate to the far field, with the rest decaying. Thus it is only those circumferential modes that propagate to the far field that represent the far-field discrete frequency noise.

The term k_ξ specifies whether a mode will propagate or not, specifically the argument under the radical. When $(k_\theta M_\theta - \omega/A_\infty)^2 - (1 - M^2_\xi) k^2_\theta > 0$, there are two real distinct axial wave numbers that correspond to two pressure waves propagating unattenuated, one upstream and the other downstream. If $(k_\theta M_\theta - \omega/A_\infty)^2 - (1 - M^2_\xi) k^2_\theta < 0$, there are two complex axial wave numbers that correspond to two decaying pressure waves, one upstream and the other downstream. With $(k_\theta M_\theta - \omega/A_\infty)^2 - (1 - M^2_\xi) k^2_\theta = 0$, there is one wave propagating in the tangential direction. This is a resonance condition, with the resonant frequency known as the cutoff frequency because below the cutoff frequency the pressure waves decay in the axial direction or are cutoff.

Mathematical Model

The blade row is modeled as a row of vortex sheets, with the vortex strength $\Gamma(x)$, and thus the unsteady pressure difference across the airfoil chord $\Delta p(x)$, $\Delta p(x) = \rho_0 W \Gamma(x)$. The term $\Delta p(x)$ fluctuates at harmonics of blade pass frequency ω and is calculated as a function of the upwash velocity $w(x)$. The upwash for the convected vortical gust and the oscillating flap and airfoil surface piston actuators (Fig. 3) are as follows.

Vortical gust:

$$w(x) = \{-w_{G,LE} \exp(-ik_c x) \quad 0 \le x \le 1\} \tag{11}$$

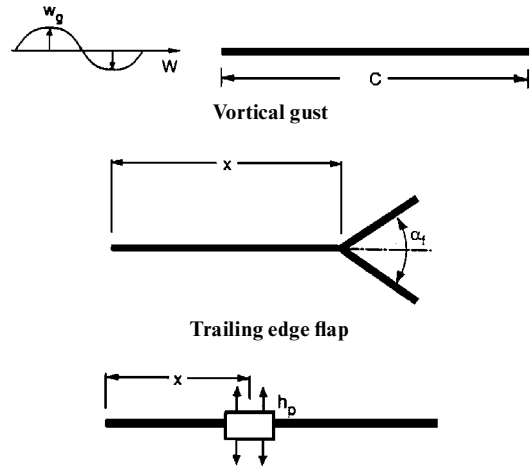

Fig. 3 Airfoil surface actuators.

Flap:

$$w(x) = \begin{Bmatrix} 0 & 0 < x < x_f \\ W\alpha_{\text{flap}}[1 - ik_c(x - x_f)]e^{i\phi} & x_f < x < 1 \end{Bmatrix} \tag{12}$$

Piston:

$$w(x) = \begin{Bmatrix} 0 & x_{P,TE} < x \\ q_{\text{piston}} e^{i\phi} & x_{P,LE} < x < x_{P,TE} \\ 0 & x < x_{P,LE} \end{Bmatrix} \tag{13}$$

The flow tangency condition on the airfoil surface, $\bar{v} = -w(x)$, is related to $\Delta p(x)$:

$$w(x) = \int_0^1 K(x - x')\Delta p(x')\, dx' \tag{14}$$

where the kernel function $K(x)$ depends on the mean flow and geometry,[8] with this equation solved for $\Delta p(x)$ and thus $\Gamma(x)$ and used to calculate the acoustic waves.

Far-Field Discrete Frequency Noise

Although all of the acoustic pressure circumferential modes of order $k_\theta = nN_{\text{blades}} + mN_{\text{vanes}}$ are generated by the rotor–stator interaction at the harmonics of blade passage frequency, only certain of these modes propagate to the far field. Thus it is only these propagating modes that represent the far-field discrete frequency noise.

If decaying perturbations are produced, the mode is cut off. For a particular set of cascade parameters, there is a definite value of $|m|$ above which all modes are cut off. For each value of m that gives a propagating mode, a pair of acoustic waves is formed, one traveling upstream and the other downstream. The upstream traveling wave is denoted by a subscript 1 and the downstream wave denoted by a subscript 2. The far-field acoustic waves generated in such a mode are determined from the bound vortex strength $\Gamma(x)$.

A bound vortex of strength $(1/S)\Gamma(x_0)\, dx_0$ creates a velocity disturbance in the tangential direction at the leading edge of the stator equal to

$$\bar{v}_{1,2} = v'_{1,2} \frac{\Gamma(x_0)}{S} \exp[-i(k_{\xi 1,2}\xi_0 + k_\theta \eta_0)]\, dx_0 \tag{15}$$

where $\bar{v}_{1,2}$ is the complex amplitude of the tangential velocity disturbance $v'_{1,2}$, $\xi_0 = x_0 \cos\Theta$, and $\eta_0 = x_0 \sin\Theta$.

The relationship between $\bar{p}_{1,2}$ and $\bar{v}_{1,2}$ is determined using the unsteady Bernoulli equation and solving Eq. (15) for the strengths of the pressure disturbances:

$$\bar{p}_{1,2} = -(\rho_0 W/k_\theta)[(k_c/C) + k_{\xi 1,2}\cos\Theta + k_\theta \sin\Theta] v'_{1,2}$$

The pressure disturbance caused by a bound vortex distribution is determined by integrating over the stator chord. Thus, the pressure disturbance at the leading edge of the stator is

$$\bar{p}_{1,2} = -\frac{\rho_0 W}{Sk_\theta}\left(\frac{k_c}{C} + k_{\xi 1,2}\cos\Theta + k_\theta \sin\Theta\right) v'_{1,2} \times \int_0^1 \Gamma(x_0)\exp[-i(k_{\xi 1,2}\cos\Theta + k_\theta \sin\Theta)x_0]\,dx_0 \qquad (16)$$

Discrete Frequency Noise Control and Cancellation

The far-field discrete frequency noise generated by rotor–stator interactions is a result of the propagating pressure or acoustic waves generated by the vortical gust convecting past the stator vane row, with the waves propagating both upstream and downstream. Hence, the far-field noise is affected through control of only the propagating pressure waves. This is accomplished by generating additional propagating pressure waves that cancel the rotor–stator generated propagating waves, thereby resulting in no propagating acoustic modes and thus no far-field discrete frequency noise.

Propagating Acoustic Wave Cancellation

The nondimensional propagating acoustic waves generated by the convected vortical gust and the oscillating control surfaces are

$$\bar{p}'_{1,2\,\text{gust}} = \frac{\bar{p}_{1,2\,\text{gust}}}{\rho_0 W W_{\text{G,LE}}} \qquad \bar{p}'_{1,2\,\text{flap}} = \frac{\bar{p}_{1,2\,\text{flap}}}{\rho_0 W^2 \alpha_{\text{flap}} e^{i\varphi}}$$

$$\bar{p}'_{1,2\,\text{piston}} = \frac{\bar{p}_{1,2\,\text{piston}}}{\rho_0 W q_{\text{piston}} e^{i\varphi}}$$

where $\bar{p}'_{1,2\,\text{gust}}$, $\bar{p}_{1,2\,\text{gust}}$, $\bar{p}'_{1,2\,\text{flap}}$, $\bar{p}_{1,2\,\text{flap}}$, $\bar{p}'_{1,2\,\text{piston}}$, and $\bar{p}_{1,2\,\text{piston}}$ are complex.

The total far-field discrete frequency noise is determined by the sum of the propagating acoustic waves. Hence, for the oscillating flap or piston,

$$\bar{p}_{1,2\,\text{total}} = \rho_0 W w_{\text{G,LE}}(\bar{p}'_{1,2\,\text{gust}}) + \rho_0 W^2 \alpha_{\text{flap}} e^{i\varphi}(\bar{p}_{1,2\,\text{flap}})$$
$$\bar{p}_{1,2\,\text{total}} = \rho_0 W w_{\text{G,LE}}(\bar{p}'_{1,2\,\text{gust}}) + \rho_0 W q_{\text{piston}} e^{i\varphi}(\bar{p}'_{1,2\,\text{piston}}) \qquad (17)$$

Ideally, the total propagating acoustic field is zero. Hence, complete cancellation of the blade row interaction generated acoustic wave by the oscillating flap or piston requires that $\bar{p}_{1,2\,\text{total}} = 0$. Thus, the following are the actuator amplitudes and phase angles for complete cancellation of the vortical gust generated propagating acoustic waves:

$$\alpha_{\text{flap}} e^{i\varphi} = -\frac{w_{\text{G,LE}}\bar{p}'_{1,2\,\text{gust}}}{W\bar{p}'_{1,2\,\text{flap}}} \qquad h_{\text{piston}} e^{i\varphi} = \frac{i w_{\text{G,LE}}\bar{p}'_{1,2\,\text{gust}}}{\omega\bar{p}'_{1,2\,\text{piston}}} \qquad (18)$$

The two complex constants that define the upstream and downstream propagating waves generated by the vortical gust $\bar{p}'_{1\,\text{gust}}$ and $\bar{p}'_{2\,\text{gust}}$ are known. Thus, for either one of these two waves, the complex motion of the flap or piston can be determined. However, note that the actuator motion required to cancel one of these waves may not be the motion required to cancel the other.

Experimental Facility and Instrumentation

The experiments were performed in the Purdue annular cascade research facility, an open-loop draw-through-type wind tunnel capable of test section velocities to 220 ft/s (Fig. 4). The flow, conditioned by a honeycomb section and an acoustically treated inlet plenum, accelerates through a bellmouth inlet to the constant area annular test section, which contains a single-stage turbomachine. The flow exiting the test section is diffused into a large acoustically treated exit plenum. The flow is drawn through the facility by a 300-hp centrifugal fan located downstream of the exit plenum. Note that the rotor that serves as a wake generator is powered to rotational speeds of over 800 rpm by a 10-hp motor.

The acoustic mode magnitudes of the spinning pressure patterns generated by the rotor–stator interaction are measured with an array of 10 Piezotronics Inc. PCB 103A piezoelectric microphones with uniform circumferential spacing, flush mounted via static pressure taps in the outer wall of the inlet annulus (Fig. 4). The microphones have a nominal sensitivity of 1500 mV/psi and a natural frequency of 13 kHz. The microphones are calibrated as installed in the rig and exhibit linear amplitude response and flat frequency response in the region of interest. Experimental error in the pressure measurement is within 3% amplitude and 5-deg phase. The microphones are located in axial planes two stator chord lengths upstream and downstream (30.48 cm, 12 in.) of the rotor. The Nyquist critical mode is 5 for the 10-microphone array, with all signals having a spatial mode order above the Nyquist critical mode aliased below the Nyquist mode.

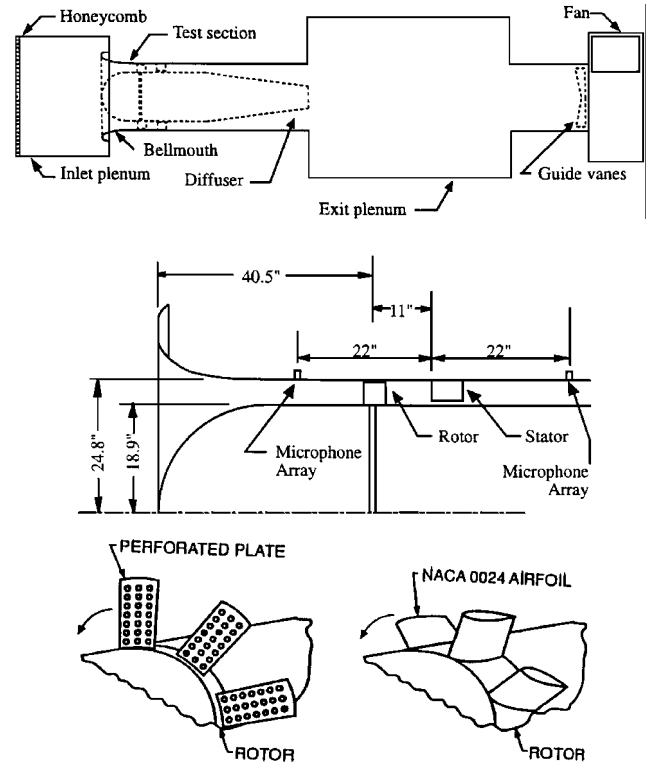

Fig. 4 Purdue annular cascade research facility and gust generators.

For these experiments, the annular test section is configured with a rotor with 16 wake generators upstream of a stator with configurations of either an isolated stator or a cascade of three stator vanes. The maximum rotor rotational speed is 800 rpm, giving the 16 rotor gust generators a rotor pass speed of 13.3 Hz and a vane pass frequency of 213.3 Hz. An optical pickup on the rotor shaft is utilized to determine the rotor pass speed.

Acoustic Modes

At blade pass frequency the cascade with 16 gust generators and a single stator generate circumferential modes of order $k_\theta = \ldots, -2, -1, 0, +1, +2, \ldots$. However, only the -1, 0, and $+1$ modes propagate when the excitation frequency is above their cut-on frequencies. For the cascade with 16 gust generators and 3 stator vanes, the circumferential modes of order $k_\theta = \ldots, -5, -2, +1, +4, +7, \ldots$ are generated, with only the $+1$ mode propagating.

Gust Generators

Two types of rotor gust generators are used to excite the acoustic modes with the downstream stator row (Fig. 4). The perforated plates generate large vortical gusts, thereby corresponding to the model forcing function (Fig. 5). The NACA 0024 rotor airfoils result in wakes an order of magnitude smaller than the perforated plate wakes, with the airfoil wake containing both vortical and potential components. The perforated plate vortical gust magnitudes are approximately 30% of the freestream velocity. These wake data are utilized to estimate the gust strengths at the various experimental operating conditions. The axial velocity and angular speed of the rotor are measured, with the velocity triangles evaluated and

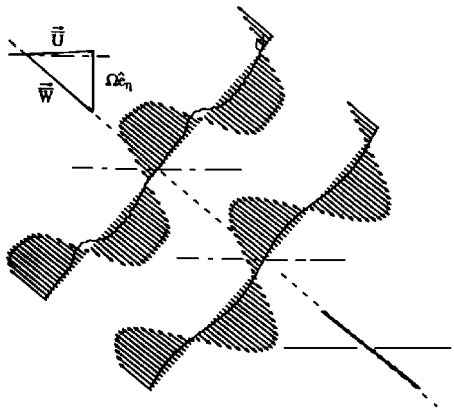

Perforated plate vortical gust

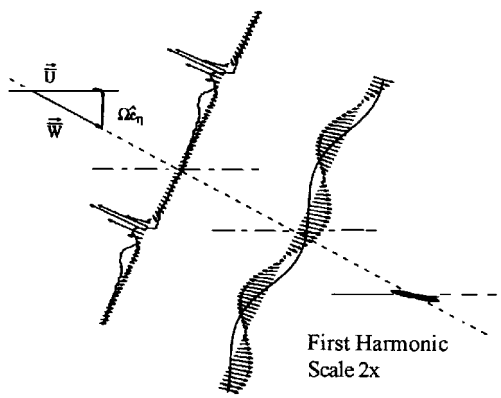

Airfoil combined potential and vortical gust

Fig. 5 Perforated plate and airfoil rotor convected gust.

the freestream velocity and direction computed. Knowing the gust strength and direction relative to the stator row, the convected gust upwash velocities along the stator vane are computed, providing the necessary gust information to model the noise experiments.

Pressure Transducers

The acoustic modes are measured with two circumferential arrays of PCB microphones installed upstream and downstream of the stator row. The PCB microphones are mounted through static pressure taps in the outer wall with uniform circumferential spacing. The PCB microphones have a resolution of 0.000022 psi,rms and a maximum pressure limit of 30 psi. This is well within the range of the acoustic modes generated in these experiments, which have a range of 0.0002–0.01 psi. Also, the response time of the PCBs is 25 μs, resulting in negligible data phase shift.

Data Acquisition

The microphone signals are measured using three National Instruments NB-A2000 analog-to-digital conversion boards with 12-bit resolution installed in an Apple Macintosh Quadra 950 computer. The NB-A2000 boards acquire data at a rate of 250,000 samples per second, taking data on four input channels simultaneously. The data acquisition is triggered with a rotor-based optical encoder signal that is in sync with rotor shaft rotation. The 10 microphone signals from either the upstream or downstream array are recorded on the three A2000 boards, with four inputs on two boards and two inputs on the third, and ensemble averaged over 400 rotor revolutions using a Labview acquisition program. The time traces are then treated as amplitude modulated signals. The spatial transform of this amplitude modulated signal yields the acoustic mode magnitudes of the pressure patterns rotating in the annulus. This data heterodyning procedure was developed by Sawyer and Fleeter.[9] Note that the upstream and downstream data are not taken simultaneously.

Airfoil and Actuator Design

Utilizing piezoelectric crystals as motor elements, two actuated airfoil designs are used, a trailing flap and a surface piston (Fig. 6).

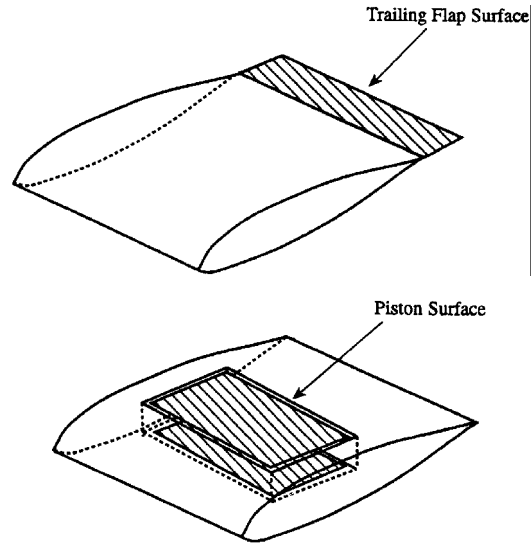

Fig. 6 Flap and surface piston actuators.

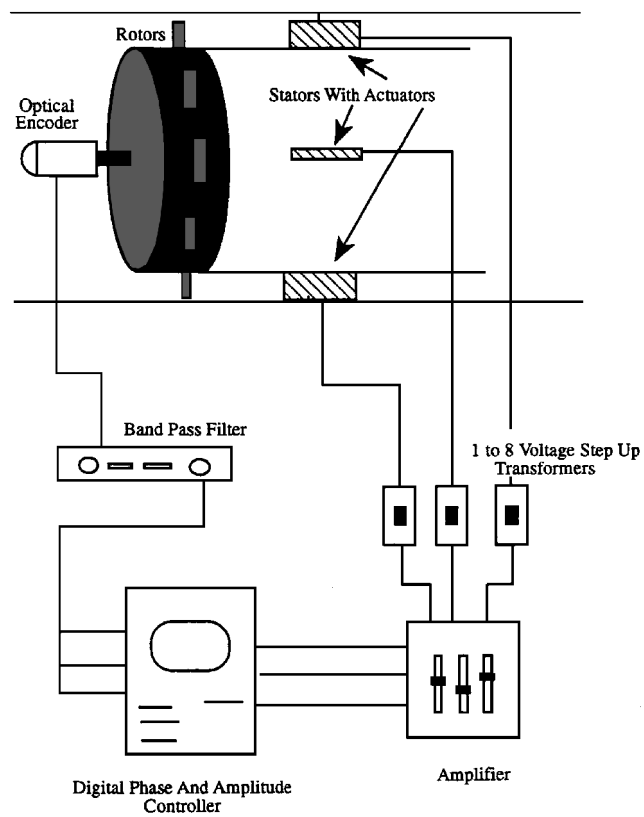

Fig. 7 Noise control system schematic.

The piezoelectric crystals are 1.5 × 2.5 in. standard two-layer piezoelectric motor elements with nickel electrodes and G1195 piezoceramic. For the flap, the piezoelectric crystal is mounted within a slot cut into the trailing edge of the stators. The crystal has a 1-in. lever arm and is sandwiched between two strips of lightweight stiff material to form the flap. The flap lengths are 15.4% of the flapped airfoil chord, with the airfoil 6.5 in. long including the flap. The piston stators have a chord length of 5.75 in. A section was removed from their center, a ledge cut at midwidth, and the piezoelectric crystal mounted with a 1-in. lever arm. A light stiff material was then used to form the surface of the 1.125-in.-long, 19.6% of the airfoil chord length, surface pistons. The piston center is located at 60.8% of the airfoil chord.

Actuator Control System

The control system for the piezocrystal actuators is depicted in Fig. 7. The piezoelectric crystals are excited by a sinusoidal varying

voltage signal generated in sync with the rotor at rotor blade pass frequency. A 16-per-revolution ±5-V square wave is generated using an optical encoder mounted on the rotor shaft. This signal is band-pass filtered to remove all but the fundamental sinusoidal signal from the square wave. This sine wave signal is then passed through an Ariel DSP-16 digital signal processor (DSP) board controlled by a second computer to control the piezocrystal excitation voltage phase and amplitude. The DSP-16 board can digitally delay a signal from 20 μs to 2621.44 ms using its buffer memory, has a 20-μs resolution, and can also control the amplitude of the delayed output signal, ranging from a minimum amplitude of zero to a maximum equal to the input voltage. The output signals from the DSP-16 boards are passed through amplified channels and then through a 1–8 step-up transformer to provide the crystals with an excitation voltage of around 680 V maximum. Operating the crystals at their maximum capacity, their off-resonance tip deflections are approximately 0.13 in. with 7.4-deg angular motion for a 1-in. lever arm, and their resonant tip deflection are from 0.15 to 0.50 in. with a range of 8.5–26.5 deg of angular motion. Measurements of the surface displacements are made using a Omron 3Z4M laser displacement sensor that has a range of 70–130 mm and a resolution of 50 μm.

Experimental Results

To both verify the basic assumptions of the math model and demonstrate active discrete frequency noise control, a series of experiments were performed in the Purdue annular cascade. The rotor was composed of 16 gust generators, either perforated plates generating a large vortical wake or airfoils that generate small wakes with both vortical and potential gust components. The noise change due to the flaps and pistons is evaluated by dividing the measured sound pressure magnitude with the actuator oscillating by the noise measured with no actuator motion, with the decibel change in noise level then evaluated, $\Delta \mathrm{dB} = 20 \log_{10}(P_{\mathrm{actuator}}/P_{\mathrm{reference}})$. The gust velocity magnitude for each case was estimated using information from Feiereisen and Fleeter,[10] with the actuator velocity magnitude evaluated considering its displacement amplitude and the frequency of the actuator motion. With regard to the experiments themselves, they were repeatable day to day, with the rotor rpm selected so as to operate the piezocrystals at resonance, thereby maximizing their amplitudes of oscillation.

Isolated Stator Vane

With 16 perforated plate or airfoil wake generators and a single stator vane, the ±1 acoustic modes propagate upstream and downstream. The actuators on the stator, either a flap or a surface piston, were then oscillated at rotor blade pass frequency to generate control propagating pressure waves that interact with the propagating acoustic waves, with the phase between the control wave and the gust variable. Note that these airfoil rotor wake amplitudes are much smaller than those generated by the perforated plate rotor. Therefore relatively large noise reductions were achieved with moderate amplitudes of the oscillating actuators.

The viability of this active noise control technique is demonstrated for a single stator vane in Figs. 8–12. The upstream and

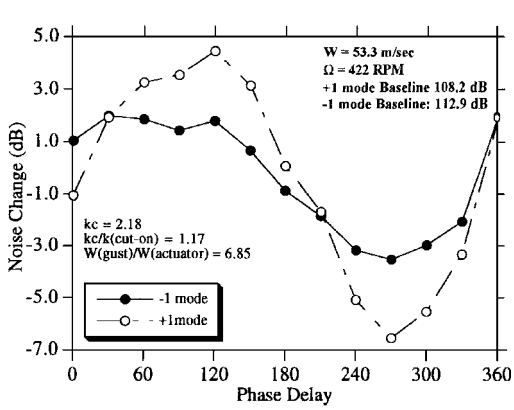

Fig. 8 Flap effect on perforated plate generated upstream propagating modes, high velocity.

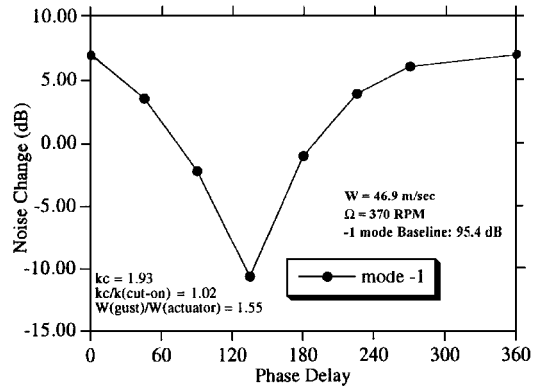

Fig. 9 Piston effect on airfoil wake single vane generated upstream propagating mode.

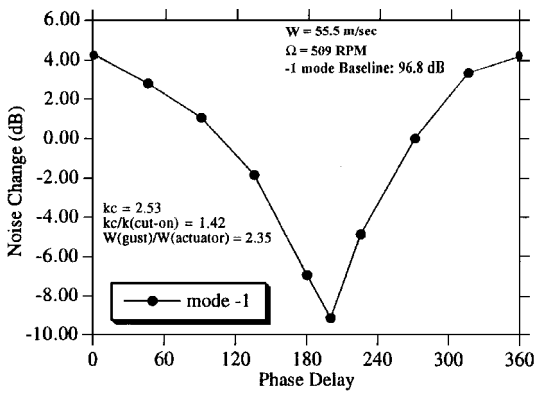

Fig. 10 Flap effect on airfoil wake single vane generated upstream propagating mode.

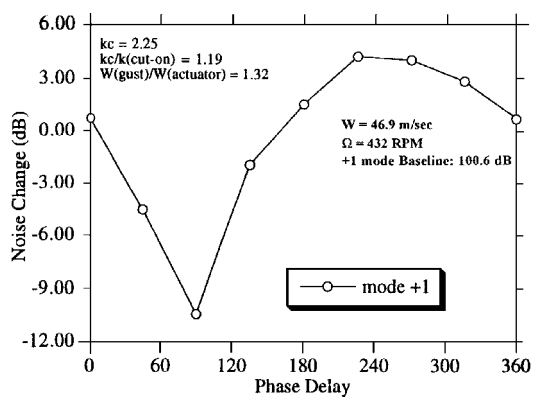

Fig. 11 Piston effect on airfoil wake single generated downstream propagating mode.

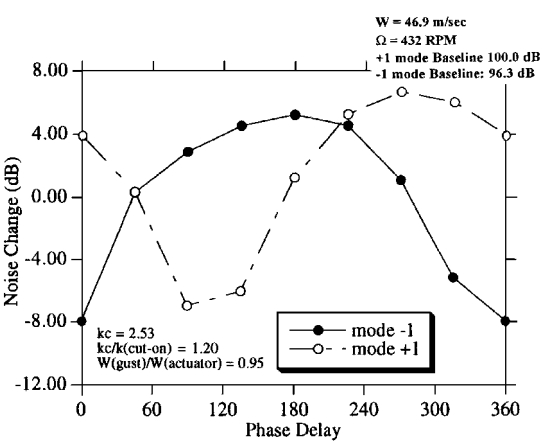

Fig. 12 Flap effect on airfoil wake single generated downstream propagating modes.

downstream propagating ±1 acoustic modes exhibit a noise increase or decrease dependent on the phase angle between the gust and the actuator, trendwise analogous to the math model predictions; i.e., the correct actuator phase angle results in a noise decrease, whereas a phase approximately 180 deg out of phase results in a noise increase.

Figure 8 shows the effect of the oscillating flap on the upstream propagating ±1 acoustic modes generated by the perforated plate rotor. A maximum decrease of nearly 7 dB for the +1 mode and 3 dB for the −1 mode are achieved, both at approximately 270-deg phase, decreasing the −1 and +1 mode noise levels from 112.9 and 108.2 dB to 109.4 and 101.6 dB, respectively. However, with a phase angle near 120 deg, the +1 mode increased by over 4 dB and the −1 mode by 2 dB. Thus, in this case, the one actuator actually acts to decrease or increase two modes simultaneously. Note that the perforated plate wakes are large, but a relatively large flap amplitude was achieved, thereby resulting in the relatively large changes in the acoustic mode amplitudes.

The effect of the piston and flap actuators on active discrete frequency noise control, with the discrete tones generated with the airfoil rotor, is shown in Figs. 9–12. The upstream propagating −1 mode is decreased by a maximum of nearly 11 dB by the piston, from 95.4 to 84.7 dB (Fig. 9), and by more than 9 dB by the flap, from 96.8 to 87.7 dB (Fig. 10). The downstream propagating +1 mode is decreased a maximum of almost 11 dB by the piston, from 100.6 to 89.8 dB (Fig. 11). In comparison, the flaps decrease this downstream propagating +1 mode by a maximum of 6.5 dB, from 96.3 to 89.8 dB, and the downstream propagating −1 mode by almost 8 dB, from 100.0 to 92.3 dB (Fig. 12). Note that no correlation with predicitons are presented for this single stator vane case because the primary interest was in the three-vane case, which is more applicable to turbomachine blade rows.

The phase angles for the maximum noise decrease are not the same for the piston and the flap actuators, as expected from the math model, which showed the importance of the location on the stator and the phase of these different actuators. For the upstream propagating −1 mode, the maximum noise reduction is found at approximately 130 deg with the piston and near 200 deg for the flap. In contrast, for the downstream propagating −1 mode, the flap phase angle for maximum noise change is close to 0 deg. With regard to the downstream propagating +1 mode, the piston and flap relative maximum noise decreases occur with a phase angle near 90 deg.

Operating the actuators at a nonoptimum phase angle results in a noise increase. For example, the maximum noise increases for the −1 mode propagating upstream are almost 7 dB for the pistons (Fig. 9) and nearly 4 dB for the flaps (Fig. 10). For the downstream propagating +1 mode, the maximum noise increase is on the order of 4 dB for both the pistons and the flaps, with the flaps increasing the −1 mode by over 5 dB (Figs. 11 and 12).

Three-Vane Stator Row

With 16 perforated plate or airfoil wake generators and a three-vane stator row, only the +1 mode propagates upstream and downstream. Oscillating stator vane actuators, either a flap or a surface piston, were oscillated at rotor blade pass frequency to generate control propagating pressure waves that interact with the propagating acoustic waves, with the phase between the control wave and gust variable.

The viability of this active noise control technique is demonstrated for the three-vane stator row with the airfoil rotor wakes in Figs. 13–15. Also shown is the correlation of these data with predictions from the model developed herein.

The flaps decrease the upstream propagating +1 mode by a maximum of almost 6 dB, from 104.0 to 98.4 (Fig. 13), and the downstream propagating +1 mode by over 8 dB, from 98.0 to 89.8 (Fig. 14). The piston actuator results in a maximum decrease in the +1 upstream propagating acoustic wave by 8 dB, from 103.4 to 95.4 dB (Fig. 15).

With regard to the phase angle for maximum tone reduction, the flaps result in maximum noise reduction near to 240 deg for the downstream propagating wave. For the upstream propagating wave, the maximum noise reduction achieved with the flaps is found at a

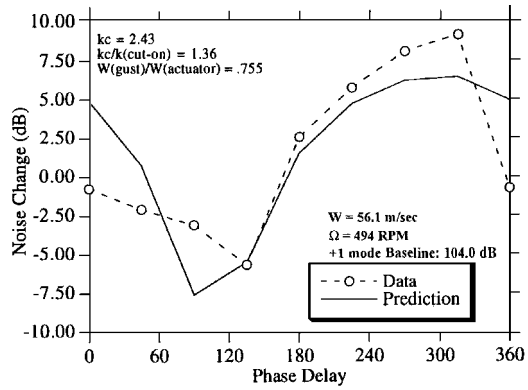

Fig. 13 Flap effect on airfoil wake vane cascade generated + 1 upstream propagating mode.

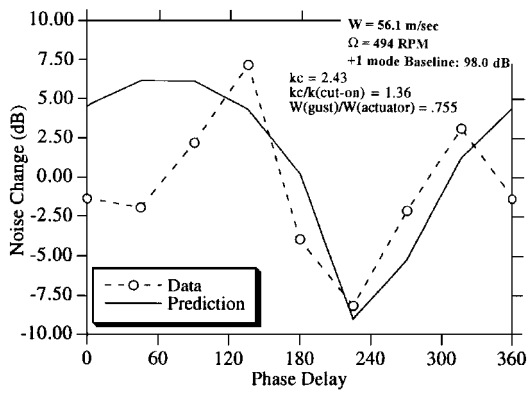

Fig. 14 Flap effect on airfoil wake vane cascade generated + 1 downstream propagating mode.

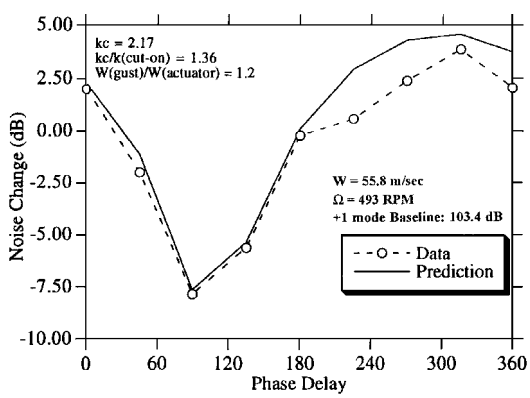

Fig. 15 Piston effect on airfoil wake vane cascade generated + 1 upstream propagating mode.

phase angle of approximately 120 deg, whereas the surface pistons result in a maximum reduction at a 90-deg phase angle. Operating the actuators at a nonoptimum phase angle results in a noise increase. For example, the maximum noise increase by the flaps for the +1 mode propagating upstream is over 9 dB (Fig. 13), with a maximum noise level for the downstream propagating mode of over 7.5 dB (Fig. 14).

For the flap actuators, the overall data–theory correlation is good, with the data and prediction both predicting approximately the same phase angle behavior and relative noise change. The noise reduction data–theory correlation is best for the downstream propagating acoustic wave, with excellent correlation obtained at the two higher reduced frequency values. For the upstream propagating acoustic wave, the data–theory correlation improves as the reduced frequency value is increased, with excellent correlation obtained at the highest reduced frequency.

Summary and Conclusions

This research was directed at active control of discrete frequency noise generated by subsonic blade rows through cancellation of the propagating acoustic waves, accomplished by utilizing airfoil mounted oscillating actuators to generate additional control propagating pressure waves. These control waves interact with the propagating acoustic waves, thereby, in principle, canceling the acoustic waves and thus the far-field discrete frequency tones. A series of experiments were described, directed at investigating the fundamentals of this active discrete frequency noise control technique as well as verifying basic math model assumptions. These experiments were performed in the Purdue annular cascade facility configured with both an isolated vane and a three-vane row, with the stator vane actuators including both oscillating flaps and surface pistons.

For a single vane, the upstream and downstream propagating ± 1 acoustic modes exhibit a noise increase or decrease dependent on the phase angle between the gust and the actuator, trendwise analogous to the math model predictions. The upstream propagating -1 mode is decreased by a maximum of nearly 11 dB by the piston and by more than 9 dB by the flap. With regard to the downstream propagation $+1$ mode, the piston achieves a maximum reduction of almost 11 dB, with the flap resulting in a 6.5-dB maximum decrease. Also, the phase angles for the maximum noise decrease are not the same for the piston and the flap actuators, as expected from the math model, which showed the importance of these different actuators and locations on the stator vane. In fact, operating the actuators at a nonoptimum phase angle results in a noise level increase.

The viability of this active noise control technique was also demonstrated for a three-vane stator row. The flaps decreased the upstream propagating $+1$ mode by a maximum of almost 6 dB and the downstream propagating $+1$ mode by over 8 dB. The piston actuators achieved a maximum decrease in the $+1$ upstream propagating acoustic wave of 8 dB. The phase angles for the maximum noise decrease are not the same for the piston and the flap actuators, with actuator oscillation at nonoptimum phase angles resulting in a noise increase.

The far-field discrete tones result from the upstream and downstream propagating acoustic modes generated by the rotor stator interaction. Both the model and experimental results show that the actuator motion that decreases one of these propagating modes may not decrease the other; in fact, it may increase it. Thus, to cancel or decrease both the upstream and downstream modes simultaneously, one actuator per propagating mode, i.e., two actuators per airfoil, is generally required.

Acknowledgments

This research was sponsored, in part, by the NASA Lewis Research Center. This financial support and the technical interchanges with Daniel Hoyniak and Daniel Buffum are most gratefully acknowledged. Also, technical discussions with Pratt and Whitney, United Technologies Research Center, and NASA Lewis Research Center with regard to these surface actuator noise control experiments are also gratefully acknowledged.

References

[1]Goldstein, M. E., *Aeroacoustics*, McGraw–Hill, New York, 1976.

[2]Hugo, R., and Jumper, E., "Controlling Unsteady Lift Using Unsteady Trailing-Edge Flap Motions," AIAA Paper 92-0275, Jan. 1992.

[3]Simonich, J., Lavrich, P., Sofrin, T., and Topol, D., "Active Aerodynamic Control of Wake-Airfoil Interaction Noise-Experiment," AIAA Paper 92-02-038, May 1992.

[4]Thomas, R. H., Burdisso, R. A., Fuller, C. R., and O'Brien, W. F., "Active Control of Fan Noise from a Turbofan Engine," AIAA Paper 93-0579, Jan. 1993.

[5]Kousen, K. A., and Verdon, J. M., "Active Control of Wake/Blade Row Interaction Noise," AIAA Paper 93-4351, Oct. 1993.

[6]Verdon, J. M., "Review of Unsteady Aerodynamic Methods for Turbomachinery Aeroelastic and Aeroacoustic Applications," *AIAA Journal*, Vol. 31, No. 2, 1992, pp. 235–250.

[7]Minter, J., Hoyniak, D., and Fleeter, S., "Oscillating Flaps for Control of Turbomachine Wake Generated Discrete Frequency Noise," *International Journal of Turbo and Jet Engines*, Vol. 11, Nos. 2–3, 1994, pp. 249–261.

[8]Smith, S. N., "Discrete Frequency Sound Generation in Axial Flow Turbomachines," Aeronautical Research Council, England, R.&M. No. 3709, 1973.

[9]Sawyer, S., and Fleeter, S., "Mean Stator Loading Effect on the Acoustic Response of a Rotating Cascade," AIAA Paper 94-2953, June 1994.

[10]Feiereisen, J., and Fleeter, S., "Low Solidity Vane Unsteady Aerodynamic Response to Combined Vortical-Potential Forcing Functions," AIAA Paper 94-2974, June 1994.

S. Glegg
Associate Editor